Collisionless Bounce Resonance Heating in Dual-Frequency Capacitively Coupled Plasmas

Yong-Xin Liu,[1] Quan-Zhi Zhang,[1] Wei Jiang,[2] Lu-Jing Hou,[3] Xiang-Zhan Jiang,[1] Wen-Qi Lu,[1] and You-Nian Wang[1,*]

[1]*School of Physics and Optoelectronic Technology, Dalian University of Technology, 116024 Dalian, China*
[2]*School of Physics, Huazhong University of Science and Technology, 430074 Wuhan, China*
[3]*Max-Planck-Institute for Extraterrestrial Physics, 85748 Garching, Germany*
(Received 6 March 2011; published 27 July 2011)

We present the experimental evidence of the collisionless electron bounce resonance heating (BRH) in low-pressure dual-frequency capacitively coupled plasmas. In capacitively coupled plasmas at low pressures when the discharge frequency and gap satisfy a certain resonant condition, the high energy beamlike electrons can be generated by fast sheath expansion, and heated by the two sheaths coherently, thus the BRH occurs. By using a combined measurement of a floating double probe and optical emission spectroscopy, we demonstrate the effect of BRH on plasma properties, such as plasma density and light emission, especially in dual-frequency discharges.

DOI: 10.1103/PhysRevLett.107.055002 PACS numbers: 52.80.Pi, 52.27.Aj, 52.65.Rr

The heating of electrons by time-varying fields is fundamental for the operation of various rf discharges [1,2]. It is now generally recognized that there are two main mechanisms for heating electrons in rf discharges: the Ohmic heating due to electron-neutral (*e*-*n*) collisions in the bulk region and the collisionless (or stochastic) heating at the oscillating plasma-sheath boundary. While the former dominates at relatively high pressures, the latter is expected to sustain the plasmas at rather low pressures, e.g., in the mTorr range. In recent years, due to the increasing emphasis on industrial applications of rf discharges in the mTorr range, the importance of understanding collisionless heating in rf discharge is growing [1–4].

In spite of decades of intensive and extensive research, the exact mechanism behind the collisionless heating and many other details are still under hot discussion [5–16]. A widespread viewpoint is that collisionless heating in rf discharges occurs in one sheath, as the electrons will undergo phase randomization when passing the bulk plasma. It was Wood [6,7] who first discovered in a particle-in-cell (PIC) Monte Carlo collision (MCC) simulation simulation that in capacitively coupled plasma (CCP) discharges fast electron beams can be created by the expanding sheaths, and these beamlike electrons can reach the opposite electrode at low pressures, then collide with the expanding sheath and are reflected back after gaining substantial energy. It is clear that this type of collisionless heating involves the cooperation of the two oscillating sheaths and that the electron motion must be coherent with the oscillation of the electric field.

This type of heating mode, now generally called bounce resonance heating (BRH), was later studied in theory by Kaganovich and others [8,9]. They showed explicitly that at low pressures the BRH occurs when the time for an electron to traverse the bulk region τ is about half the rf period or its odd times, i.e., $\tau \approx n\tau_{\rm rf}/2$, where $\tau_{\rm rf}$ is one rf period and $n = 1, 3, 5, \ldots$, and it is most effective at $n = 1$ [8]. They predicted that for a fixed discharge frequency there exists a certain discharge gap at which the plasma resistance or equivalently the electron heating reaches the maximum [9]. The BRH condition was then confirmed by Park *et al.* [10] using PIC MCC simulation, in which they observed that the BRH leads to a plateau in the electron energy probability function (EEPF) in the low energy regime (1–3 eV). However, this energy is too small to affect the overall discharges. Recently Jiang *et al.* [14] investigated the gap effect by using PIC MCC simulations and they observed an enhancement of plasma density around a certain gap, but they did not explain why.

Schulze *et al.* [13] had discovered in CCP experiments that high energy electron beams are produced by a fast expanding sheath and bounce between two sheaths. However, this bouncing is not a resonant bouncing. In CCPs, You, Chung, and Chang [11] had experimentally observed a low energy electron BRH, but this electron cannot affect plasma properties. A similar electron BRH had also been observed in experiment by Chung *et al.* [12], but in inductively coupled plasmas.

Up to now, however, there has not been any experimental observation about high energy electron BRH in CCPs, especially in dual-frequency (DF) CCPs. In this Letter, we conduct a combined experimental and numerical study of the BRH in a DF CCP discharge with argon, present the experimental evidence of the BRH in CCPs and its effect on plasma density, light emission, and EEPFs, and demonstrate the different behavior of BRH in single-frequency (SF) and DF discharges.

Our experiment was performed in a parallel plate DF discharge chamber [17]. The ion (plasma) density at the discharge center was measured by utilizing a complete floating double probe technique [17], and the electron excitation was measured by optical emission spectroscopy at the line of 811.4 nm. We paid particular attention to the dependence of plasma density and light intensity on the gap length L (varying from 1.25 to 6 cm), low frequency (LF) power P_L (varying from 150 to 0 W) and LF F_L (varying from 1.5 to 2.5 MHz), while the high frequency (HF) and power are fixed at 60 MHz and 50 W, respectively. Our simulation was based on the standard 1d3v PIC MCC method [14], in which the electrode at $x = L$ was grounded and the one at $x = 0$ was driven by a DF voltage source, whose waveform was from the experimental measurements.

The most direct effect of the BRH was observed from an anomalous increase of the plasma density and light intensity with the decrease of L as shown in Fig. 1. We see in both experiment and simulation that the plasma density decreases first with the decrease of L; however, a hill then builds up around $L = 2.25$ cm (to be denoted as L_{BRH} hereafter), at which the time for the electron beam to traverse the bulk is roughly half a HF period, corresponding to the BRH condition. Although, in general, the light intensity decreases with the increase of L, a pronounced peak coinciding with L_{BRH} can be easily identified, clearly indicating an enhanced electron heating at L_{BRH}.

We next did an analysis based on PIC MCC simulations to reveal the physics of the BRH. In Fig. 2, we demonstrate the ionization rates and waveforms of sheath edges at L_{BRH}, together with the trajectory and kinetic energy of a typical resonant electron. Inspecting Fig. 2(a) together with Fig. 2(b), we see that the strongest ionization happens always in the phases of the fastest sheath expansion. At these phases, some bulk electrons collide with the expanding sheath and are bounced back into the bulk like a beam. These electrons typically have an energy of about 8 eV right before joining the resonance in the case shown here. So there is actually a minimum kinetic energy $\varepsilon_{\min}$ that is needed for an electron to join the resonance with sheath oscillation. And a resonance is often started with an *e-n* elastic collision, which assigns large axial momentum to the electron so that it can penetrate into the sheath and collide with the sheath more efficiently. The resultant high energy beamlike electrons produce an intensive ionization while traversing the bulk to the other electrode and their trails can be easily identified from the highlighted ionization zone connecting the two sheath edges. Interestingly those residual beamlike electrons, which suffer no collisions during this course, arrive at the other sheath at its fastest expansion phase too. Therefore these electrons, together with many other new ones, are bounced again back into the bulk, after gaining typically a few eV during the collision with the expanding sheath. We observed that a substantial amount of electrons (about 1% for L_{BRH} at 1.3 Pa in one LF period) can bounce back and forth between two sheath edges like ping-pong balls for typically a few HF periods. The trajectory of a typical resonant electron is also shown in Fig. 2(a), and we see together with Fig. 2(c) that it gains energy in each collision with the expanding sheaths between 0 and 2.4 HF periods.

There are many channels through which a resonant electron can be deresonated. First, it could lose much energy through inelastic collisions, producing excitation or ionization, and becomes out of phase with rf oscillation. This is exactly how the BRH deposits energy to plasmas,

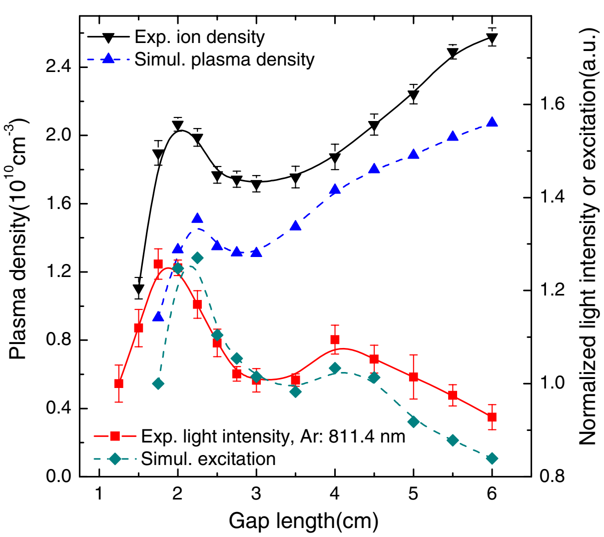

FIG. 1 (color online). Plasma density and light intensity versus L, both measured at the center of the discharge gap at a fixed power. Solid lines are from experimental measurements at 0.7 Pa, while dashed lines are from simulations at 1.3 Pa. Note here that the light intensity is normalized by the value at the smallest gap length.

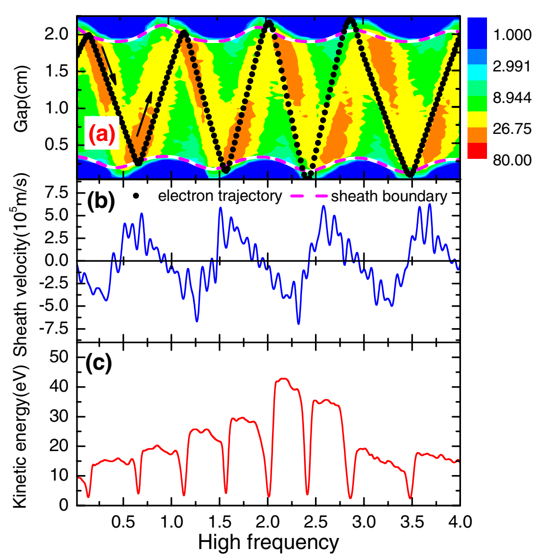

FIG. 2 (color online). (a) Spatial-temporal evolution of ionization rates (unit in 10^{20} m^{-3} s^{-1}) (contours) in 4 HF periods from simulations at 1.3 Pa and $L_{\mathrm{BRH}} = 2.25$ cm, together with variations of sheath edges (dashed lines) at both electrodes and the trajectory (dots) of a typical bouncing electron. The sheath region in the simulation is defined by $E > 100$ V/m, (b) the corresponding expanding speed of the powered sheath (by numerical differentiation of the sheath edge), and (c) the variation of the kinetic energy for the corresponding electron.

and causes the enhanced ionization and excitation in Fig. 1. Second, it could gain too much energy, so that it reaches the other sheath edge at its collapsing phase and gets deaccelerated, such as the electron that is shown here between 2.4 and 4.0 HF periods in Fig. 2(c). The second loss mechanism is important because it actually places an upper bound of energy $\varepsilon_{\rm max}$ that a resonant electron can obtain during consecutive heating. For $L_{\rm BRH}$, we have $\varepsilon_{\rm max} \approx 50$ eV, where an obvious knee point can be seen in corresponding EEPFs in Fig. 3. Third, a resonant electron could lose a large part of its axial momentum during an elastic collision and become out of phase with rf. We have actually observed a suppression of BRH at higher pressure in both experiment and simulation. Fourth, it could gain enough energy and escape from the sheath barrier, as will be discussed below in more detail.

Figure 3 shows EEPFs for, respectively, $L = 1.75$, 2.25, 3, and 4 cm under the same conditions as in Fig. 1. One can see that the EEPFs can roughly be divided into two regions at about $\varepsilon \approx 20$ eV, i.e., a low energy region at $\varepsilon < 20$ eV and a high energy region at $\varepsilon > 20$ eV, respectively. In the former, the EEPFs exhibit a typical bi-Maxwellian structure that is quite similar to the usual EEPFs observed in bulk plasmas. In the high energy region, we observe many extended high energy tails in the EEPFs, due to the contribution from high energy resonant electrons. Taking the case of $L_{\rm RBH}$, for example, we see that the high energy tail starts at around 25 eV and lasts till about 50 eV, at which there appears a knee point. It is now not a big surprise that this knee point coincides with $\varepsilon_{\rm max}$, beyond which the resonant electrons are deresonated. The similar structures are also seen in other EEPFs, but with different $\varepsilon_{\rm min}$ and $\varepsilon_{\rm max}$. A particularly interesting case is $L = 1.75$ cm, at which the high energy tail actually starts quite early at about $\varepsilon \approx 7$ eV, but ends early too (so $\varepsilon_{\rm max} \approx 20$ eV). There are actually many more resonant electrons in this case; however, these electrons become out of phase with a rf period at rather low $\varepsilon_{\rm max}$ and cannot contribute much to ionization or excitation. At larger gaps, both $\varepsilon_{\rm min}$ and $\varepsilon_{\rm max}$ increase, and this leads to a competitive situation for the RBH. On one hand, an increase of $\varepsilon_{\rm min}$ places a more difficult initial condition for electrons to join the resonance. On the other, an increase of $\varepsilon_{\rm max}$ means a higher energy that a resonant electron can obtain. So the balance of the two factors determines the heating of the plasmas to be the most significant at $L = 2.25$ cm.

Although the energetic beamlike electrons are resonantly heated by HF oscillating sheaths, the LF source has very significant effects on the BRH. First, we adjust the P_L from 50 to 0 W in experiment, and observe a dramatic change of the light emission in both its intensity and profile, as is shown in Fig. 4(a). There is only one prominent resonance peak at $P_L = 50$ W; however, with the decrease of P_L another peak in the excitation emerges at a much smaller gap $L \approx 1.25$ cm, while the main peak diminishes gradually. From 20 to about 5 W, the two peaks coexist. And when it reaches $P_L = 0$, in a SF discharge, the main peak at $L_{\rm BRH}$ totally disappears, whereas the peak at the smaller gap outstands it. We next tune the F_L in a range that is allowed by our experimental setup. We see there is a clear tendency that with the decrease of F_L the resonance peak is shifting gradually towards a smaller gap, as is shown in Fig. 4(b), while the intensity increases. Although we cannot see the complete transition for F_L smaller than 1.5 MHz, due to the experimental constraint, we can infer that the light emission curve should converge to one that is quite similar to $P_L = 0$ shown in Fig. 4(a)

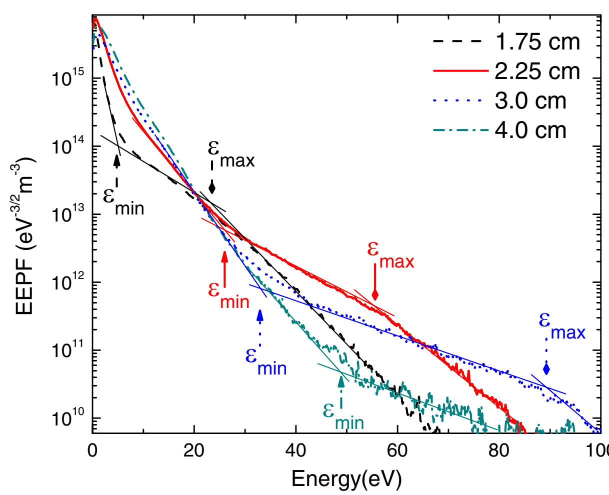

FIG. 3 (color online). EEPFs from simulations at 1.3 Pa for, respectively, $L = 1.75$ cm (dashed line), 2.25 cm (solid line), 3.0 cm (dotted line), and 4.0 cm (dash-dotted line). It should be remembered here that the full space EEPFs are adopted.

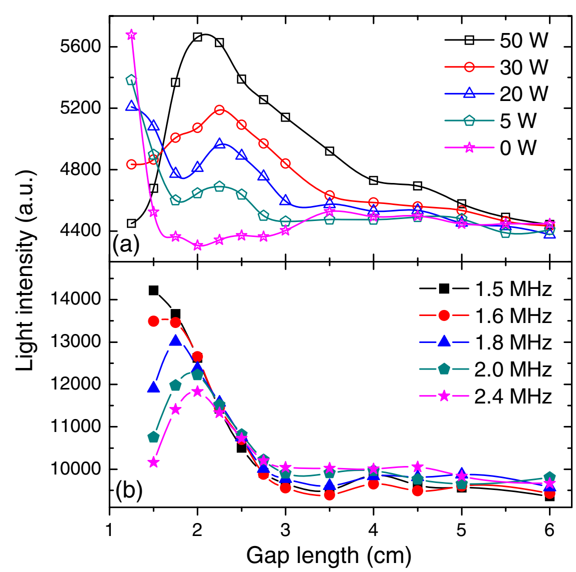

FIG. 4 (color online). Experimental measurements of light intensity versus L: (a) at different LF powers for fixed F_L of 2 MHz and (b) at different low frequencies for fixed P_L of 100 W, 0.7 Pa.

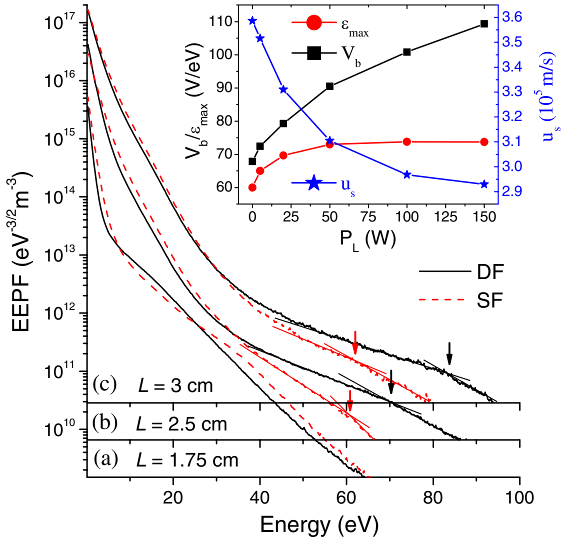

FIG. 5 (color online). EEPFs from simulations at 1.3 Pa for, respectively, (a) $L = 1.75$ cm, (b) 2.5 cm, and (c) 3.0 cm. For clarity, the lines are shifted by 15% from bottom to top. Red dashed lines are from SF discharges, while black solid lines are from corresponding DF cases (P_L of 150 W). The inset shows the averaged sheath barrier voltage V_b, ε_{max} in the EEPFs of DF discharges, and the averaged sheath speed u_s, respectively, for a fixed gap length $L = 2.5$ cm but different LF powers.

when F_L goes to zero. Both these experiments suggest that the BRHs in SF and DF discharges behave quite differently.

What we can only infer so far is that the LF component has greatly changed the sheath properties. As evidence, we clearly observe from simulation that there is an increase of sheath thickness and consequently a decrease of bulk length with the increase of F_L and P_L. This may explain the fact that the most significant enhancement due to BRH tends to occur at a relatively larger L for higher F_L and P_L, as is shown in Fig. 4.

To shed further light on the differences of BRH in SF and DF discharges, we show in Fig. 5 comparisons of the EEPFs between SF and DF discharges for different gap lengths and LF powers, obtained from PIC MCC simulations. Generally we see a larger influence of P_L on the shape of the EEPFs of larger L, e.g., $L = 2.5$ cm and 3 cm. Interestingly, the knee points ε_{max} in SF discharges are always at around 60 eV, whereas in the cases of DF they increase with the increase of L, as we had already seen in Fig. 3. This can be understood as follows: in SF discharges the ε_{max} is mainly restricted by the sheath barrier voltage V_b, and since V_b does not change much for different gap lengths, we see the knee point hardly moves at all for different gap lengths. However, in the case of DF discharges, it is L that mainly decides the ε_{max}, since the V_b is much larger than the ε_{max}, as is shown in the inset of Fig. 5, which exhibits effects of P_L on the sheath properties for $L = 2.5$ cm. We can see that sheath barrier voltage increases monotonously with the increase of P_L, while ε_{max} increases and reaches a plateau at about $P_L = 50$ W. In particular, when $P_L = 0$, so in a SF discharge, V_b and ε_{max} become quite comparable.

In summary, we have presented the experimental evidence of the so-called collisionless electron BRH in low-pressure DF CCPs. Our simulations not only reconfirm the experimental observation, but reveal many more details about the mechanism and behavior of the BRH in both SF and DF discharges. We observe that the BRH can significantly enhance the ionization or excitation rate in the discharge and consequently increase the plasma density, and the BRH is most prominent at low pressures. In particular, we have found that the resonance frequency and the resonance discharge gap satisfy very well the following relation: $f_{\rm BRH} L_{\rm BRH} \approx 150$ MHz $\cdot$ cm. In addition, we have found that the BRH behaves quite differently in SF and DF discharges. Generally speaking the BRH in DF tends to occur in a larger discharge gap than in SF cases, and the BRH is more effective in DF discharges. The reason may lie in the fact that the LF component can change the sheath properties, such as the sheath expansion speed and sheath barrier voltage in a subtle yet fundamental way.

This work was supported by the National Natural Science Foundation of China No. 10635010, the National Basic Research Program of China No. 2010CB832901, and the Fundamental Research Funds for the Central Universities (Grant No. DUT11ZD109).

*ynwang@dlut.edu.cn

[1] M. A. Lieberman and A. J. Lichtenberg, *Principles of Plasma Discharges and Materials Processing* (Wiley, New York, 2005).
[2] M. A. Lieberman and V. A. Godyak, IEEE Trans. Plasma Sci. **26**, 955 (1998).
[3] V. A. Godyak, R. B. Piejak, and B. M. Alexandrovich, Phys. Rev. Lett. **68**, 40 (1992).
[4] M. M. Turner and P. Chabert, Phys. Rev. Lett. **96**, 205001 (2006).
[5] H. C. Kim and J. K. Lee, Phys. Rev. Lett. **93**, 085003 (2004).
[6] B. P. Wood, PhD thesis, University of California, Berkeley, 1991.
[7] B. P. Wood, M. A. Lieberman, and A. J. Lichtenberg, IEEE Trans. Plasma Sci. **23**, 89 (1995).
[8] Y. M. Aliev, I. D. Kaganovich, and H. Schlüter, Phys. Plasmas **4**, 2413 (1997).
[9] I. D. Kaganovich, Phys. Rev. Lett. **89**, 265006 (2002).
[10] G. Y. Park *et al.*, Phys. Rev. Lett. **98**, 085003 (2007).
[11] S. J. You, C. W. Chung, and H. Y. Chang, Appl. Phys. Lett. **87**, 041 501 (2005).
[12] C. W. Chung *et al.*, Phys. Plasmas **8**, 2992 (2001).
[13] J. Schulze *et al.*, IEEE Trans. Plasma Sci. **36**, 1400 (2008).
[14] W. Jiang *et al.*, J. Phys. D **42**, 102 005 (2009).
[15] E. Kawamura, M. A. Lieberman, and A. J. Lichtenberg, Phys. Plasmas **13**, 053 506 (2006).
[16] T. Mussenbrock *et al.*, Phys. Rev. Lett. **101**, 085004 (2008).
[17] X. Z. Jiang *et al.*, J. Vac. Sci. Technol. A **29**, 011 006 (2011).